CRIMSON PUBLISHERS
Wings to the Research

Research in
Medical & Engineering Sciences

ISSN: 2576-8816

Short Communication

Honey Mediated Green Synthesis of Photoluminiscent Zns Nano/Micro Particles

Esakkiammal A, Malathi A, Ujjal Kumar Sur* and Balaprasad Ankamwar*

Department of Chemistry, India

***Corresponding author:** Ujjal Kumar Sur and Balaprasad Ankamwar, Bio-Inspired Materials Research Laboratory, Department of Chemistry, Pune-411007, India

Submission: November 15, 2017; **Published:** January 23, 2018

Abstract

Honey, a common natural product contains biomolecules responsible for the reduction and stabilization of nanoparticles. In this paper, we have demonstrated the cost effective, eco-friendly green synthesis of zinc sulphide nano/microstructures by chemical co-precipitation method using honey as the stabilizing agent. The structural and morphological properties of zinc sulphide nano/microstructures were studied by X-ray diffraction, scanning electron microscopy, energy dispersive X-rays spectroscopy and Fourier transform infra-red spectroscopy. Comparative studies on the synthesized zinc sulphide nano/microstructures before and after calcinations (700 0C) were carried out using UV-visible and photoluminescence spectroscopy. UV-visible spectroscopy data shows that there is blue shift of the absorption peak for the synthesized zinc sulphide nano/microstructures sample (Eg=4.08 eV) and red shift of the absorption peak for the calcinized (700 oC) sample (Eg=3.37 eV) with respect to bulk sample. X-ray diffraction data reveals that phase transformation has occurred after calcination from cubic zinc blende structure to hexagonally packed wurtzite structure and it is also partially oxidized to zinc oxide.

Keywords: Zinc sulphide; Calcinations; Honey; Zinc oxide; Wurtzite; Zinc blende

Introduction

Zinc Sulphide (ZnS), a direct wide band gap, (II-VI) group, optically transparent semiconductor [1,2] has gained great importance as phosphor material for fabricating photoluminescence, electroluminescence as well as luminescence devices [3]. ZnS can be widely utilized in photonics, optoelectronics with diverse applications such as optical coatings, field effect transistors, sensors, transducers and in many other optoelectronic devices such as blue-emitting diodes, electroluminescence devices and solar cells. ZnS exhibits a wide band gap (Eg=3.66 eV) [4], which is responsible for its fascinating properties and potential diverse applications in optical devices. The most important feature of ZnS nanostructure is its amazing physical and chemical properties, which are drastically differ from that of bulk semiconductor, i.e. ZnS nanostructure exhibits wider band gap and quantum size confinement.

ZnS crystallizes into two allotropic forms; zinc blende or sphalerite which can exist in cubic form and wurtzite which can exist in hexagonal close packing form [3,5,6]. Among these two structures, cubic form is stable low temperature phase [7]. ZnS of different sizes and shapes can be prepared in the form of thin films, powders and colloids using techniques such as solvothermal [8,9], chemical vapour deposition (CVD) [10], chemical precipitation [11], microwave radiation [12,13], mechano-chemical synthesis etc [14]. ZnS nanostructures can be prepared via different protocols, including solid-state reaction, sol-gel process and hydrothermal method.

Nanobiotechnology, a new branch of nanotechnology can provide an economically viable and environmental friendly green synthetic protocol alternative to commonly used chemical and physical method of nanoparticles synthesis. Nanomaterials can be synthesized using microorganisms, including bacteria, viruses, fungi as well as plant and animal based products. A wide variety of metal nanoparticles had been synthesized using microorganisms [15,16], as well as plant and fruit extracts [17-20].

Honey, a natural sweetener can be produced by bees using nectar from flowers. It contains several biomolecules responsible for the reduction and stabilization of nanoparticles from metal salts precursors and has been exploited by several groups for the synthesis of metal nanoparticles including gold, silver, palladium and platinium [21-24]. Still, there is much more space for the improvement in bio-based methods of synthesis for metal and semiconductor nanoparticles. Although, ZnS nanoparticles had been biogenically synthesized recently using edible mushroom *Pleutotuss ostreatu* [25], it has not yet been prepared using honey. In this paper, we have described the green synthetic protocol for the preparation of ZnS nano/microstructures using honey as the stabilizing agent. As per our knowledge, this is the first instance of

biosynthesis of ZnS nanostructures from honey. The biosynthesized semiconductor nano/microstructures were characterized by X-ray diffraction, scanning electron microscope, energy dispersive X-rays spectroscopy and Fourier transform infra-red spectroscopy. Comparative studies on the synthesized zinc sulphide nano/microstructures before and after calcinations (700 0C) were carried out using UV-visible and photoluminescence spectroscopy to determine the stability and structure of ZnS.

Experimental

Zinc acetate dihydrate ($C_4H_6O_4.Zn.2H_2O$) and sodium sulfide (Na_2S) were used as precursors in our synthesis, which were obtained from Sigma Aldrich. Honey was used as stabilizing agent in our synthetic protocol. All the aqueous solutions were prepared using Millipore water.

For the green synthesis of ZnS nano/microstructures, freshly prepared aqueous solution of zinc acetate dihydrate (0.1gm) and sodium sulphide (0.85gm) were used at room temperature. To the mixture of aqueous solution of zinc acetate dihydrate and honey, solution of sodium sulphide was added dropwise with continuous stirring at 2000rpm resulting in the formation of white precipitate. Stirring was continued for 30 minutes for the completion of the reaction. The product obtained in the form of white precipitate was centrifuged and washed twice with Millipore water and dried naturally. One part of the biosynthesized ZnS sample was calcinated at 700 oC. The synthesis process can be summarized by the chemical equation given below

$$Zn(C_2H_3O_2)_2 + Na_2S \xrightarrow{Honey} ZnS + 2NaC_2H_3O$$

The morphology of the synthesized ZnS sample was studied using a (JEOLJSM-6360A) scanning electron microscope (SEM) and the purity and elemental analysis was carried out using energy dispersive X-ray spectrscopy (EDAX). The crystal structure of the synthesized sample before and after calcinations at 700 0C was studied by X-ray Diffraction (XRD) using a D8 Advanced Bruker instrument with CuK_α radiation (1.54 Å) at the scanning rate of $1min^{-1}$. Fourier transform Infra-red (FTIR) analysis of the samples were recorded over 4000 to $400cm^{-1}$ wave number region with Bruker (Vector 22) mid-IR spectroscopy (Bruker, Germany). Absorption spectra were recorded using a Perkin-Elmer (Lambda-950) UV-Vis NIR spectrophotometer. The photoluminescence spectra were obtained using a (Shimadzu-2100) fluorescence spectrophotometer.

Results and Discussion

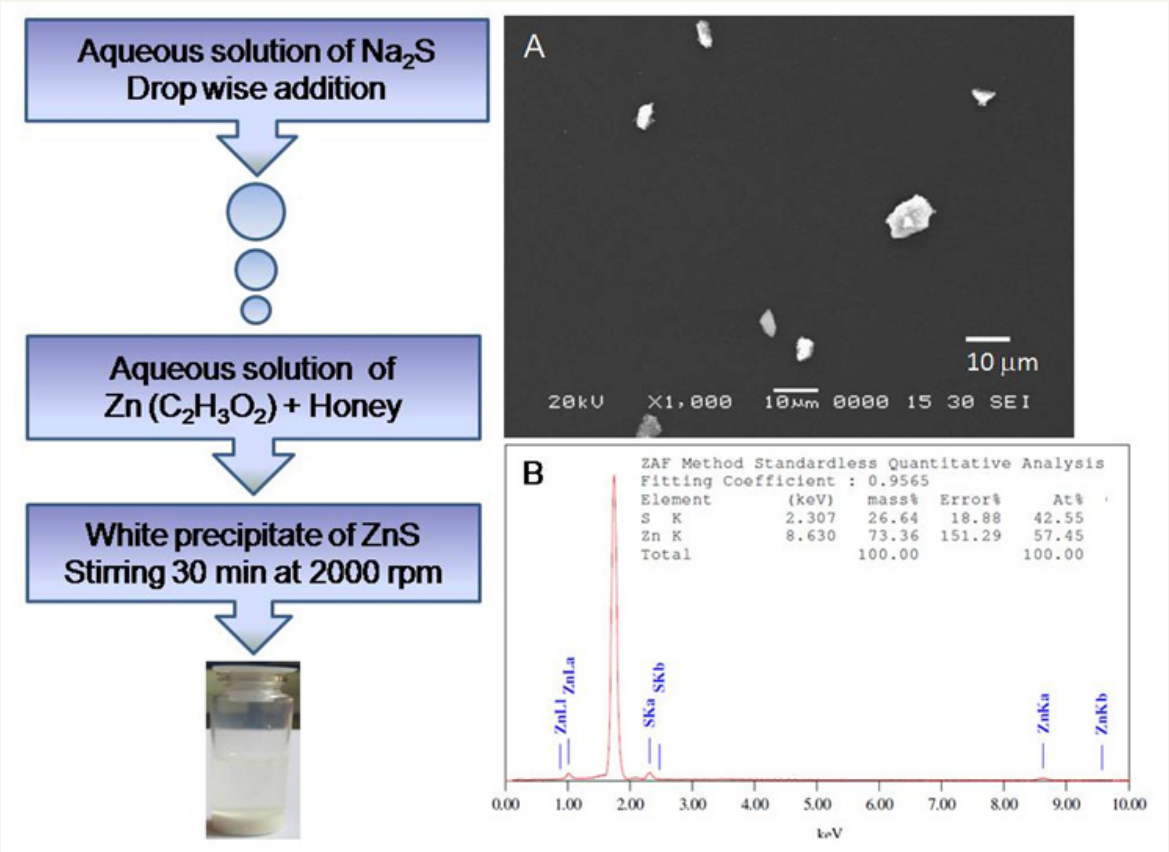

Figure 1: The SEM image as well as the EDAX spectrum of as synthesized honey-mediated ZnS sample.

The morphology as well as the structure of the biosynthesized ZnS obtained from honey was determined using SEM.One part of the synthesized ZnS sample was calcinated at 700 0C (Figure 1A & 1B) illustrates the SEM as well as the EDAX spectrum of as synthesized ZnS sample. As shown from the SEM image in Figure 1(A), both micro and nanoparticles were obtained.

The EDAX spectrum shown in Figure 1(B) indicates that there are clear peaks for zinc and sulphur with the composition of the honey mediated biosynthesized sample is mainly zinc (57.45 at%) and sulphur (42.55 at %).

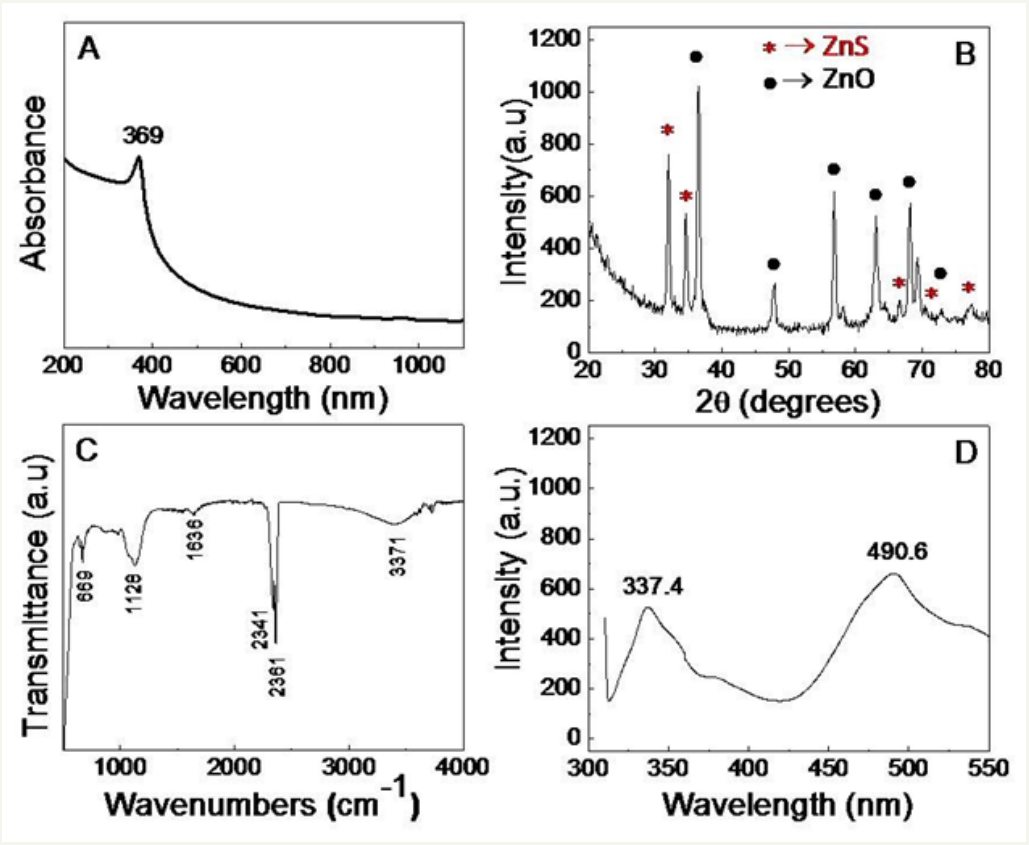

Figure 3: (A) The UV-visible absorbance spectrum; (B) The XRD pattern; (C) The FT-IR spectrum, and (D) The Photoluminescence spectra of biosynthesized honey-mediated ZnS nano/microstructures after calcination at 700 oC.

Figure spectra

Figure the honey Figure 2A, fairly a blue shift from the absorption edge of the bulk ZnS sample at 345nm. The band gap energy (Eg in eV) calculated from the absorption data was found to be 4.08eV. This signifies the reduction of particle size with widening in the band gap energy compare to bulk value of 3.66 eV, which can be explained by the quantum confinement effect [2].

The XRD pattern of our synthesized ZnS sample is shown in Figure 2B. Three diffraction peaks were obtained with 2θ values 28.73°, 48.02° and 56.90° corresponds to (111), (220) and (311) planes respectively signifies of sphalerite or zinc blende structures of ZnS (JCPDS no. 05-0566), which confirms the purity of the sample and suggests that the sample is in the cubic form of zinc blende structure [26]. The average crystallite size (D) of the ZnS sample was calculated using the classical Scherrer formula: [27,28]

$$D = \frac{k\lambda}{\beta \cos\theta} \quad \text{--- (1)}$$

where, the constant k is the shape factor usually equal to 1, λ is the wavelength of X–ray, β is the Bragg's angle and β is the full width of the half maxima (FWHM). The average crystallite size of as

biosynthesized ZnS particles to find out the presence of different functional groups of biomolecules in honey, which are responsible for the stabilization of ZnS nano/microstructures. Figure 2C shows the FTIR spectra in the range of 4000-400cm1. The significant vibration peaks observed [26,29-31] at 470, 617, 669 and 1022cm-1 are due to symmetric bending arising from Zn-S vibration. Peaks obtained at 1340 & 2341cm^{-1} is due to adsorption of atmospheric CO2 on the surface of the synthesized particles [26,30]. The peaks in the range of 3000-3600cm^{-1} are attributable to O-H stretching frequency which indicates the presence of water adsorbed on the surface of the ZnS particles. The water was probably introduced from the atmosphere during FTIR analysis. Proteins present in honey can either bind through free amine group or carboxylate ion (-COO-) residue present in it. A weak band at 1716cm^{-1} is characteristic of the C=O stretching mode of carboxylic acid. Amide I and amide II are the two prominent IR bands of the proteins. The IR bands around 1647cm1arise from amide Idue to the stretching vibrations of the C=O and C-N groups and band at 1541cm^{-1} is from amide II mainly due to N-H bending. Peak observed at 1022cm^{-1} is from C-O-C symmetric stretching vibration of proteins [21,22].

Photoluminescence spectra of ZnS sample is demonstrated in Figure 2D. As shown in the Figure, the plot contains two peaks at 334.6 and 423.8nm for ZnS sample. Appearance of a broad peak centered at 423.8nm can be attributed to the presence of sulphur vacancies in the lattice [6]. The other peak at 334.6nm is due to the band to band transition of ZnS.

XRD and FTIR studies were carried out on the biosynthesized ZnS sample after calcinations of at 700 0C. Similarly, comparative studies on the synthesized zinc sulphide nano/microstructures before and after calcinations (700 0C) were carried out using UV-visible and photoluminescence spectroscopy. Figure 3A shows the UV-visible spectrum of ZnS sample after calcination. The absorption peak after calcinations at 700 0C appeared at 369nm, which clearly exhibits a red shift from the absorption edge of the bulk ZnS. The band gap energy (Eg in eV) calculated from the absorption data was found to be 3.37eV for the ZnS sample after calcinations at 700 oC.

Figure 3B represents XRD pattern for calcinized sample at 700 °C, it shows the diffraction peaks obtained at 2θ values are 32°, 34.7°, 66.4°, 70.3°, and 77.5° corresponding to the (105), (106), (016), (011), and (214) planes of ZnS according to JCPDS (card no: 72-0163) reveals that ZnS has hexagonal packed wurtzite structure [29] and the values 36.5°, 47.9°, 56.8°, 63.1°, 68.2°, 72.8° corresponding to the (101), (102), (110), (103), (112), (004) planes of ZnO according to JCPDS (card no: 75-0576) [32,33].

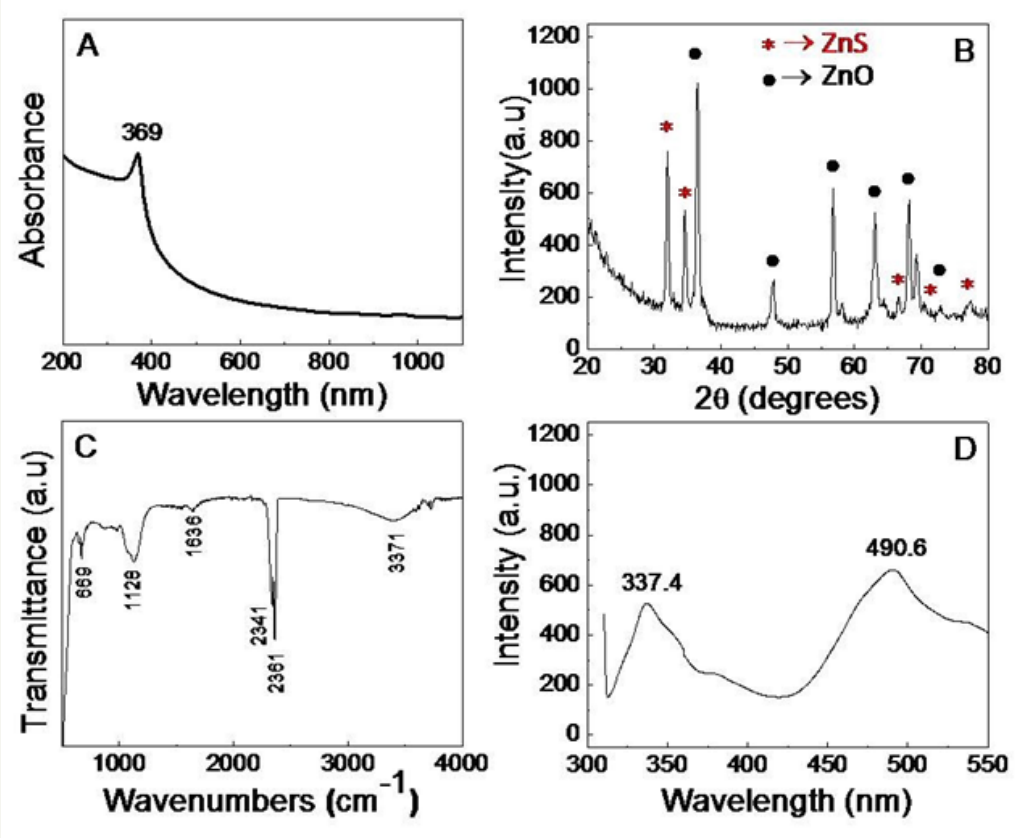

Figure 3: (A) The UV-visible absorbance spectrum; (B) The XRD pattern; (C) The FT-IR spectrum, and (D) The Photoluminescence spectra of biosynthesized honey-mediated ZnS nano/microstructures after calcination at 700 oC.

This result indicates that the ZnS sample can get transformed from the cubic zinc blende structure to hexagonal packed wurtzite structure and part of it gets converted into zinc oxide (ZnO). The average crystallite size of the calcinated ZnS sample at 700 oC, corresponding to ZnS crystallites as estimated from XRD was 21.2nm and that for ZnO crystallites, the estimated value was 36.4nm. Therefore, it can be seen that the calcinations effects will contribute towards the improvement of crystallite size, which may be due to recrystallization effects at higher calcinations temperature [34]. This indicates that the higher calcinations temperatures may lead to complete conversion of ZnS in to ZnO. The possible oxidation reaction for conversion of ZnS in to ZnO is as given below in which sulfur dioxide gas is released as a byproduct. The oxygen required for reaction if taken from air.

$$2ZnS_{(solid)} + 2O2_{(Gas)} (> 700\ oC) 2\ ZnO_{(solid)} + SO_2\uparrow_{(Gas)}$$

Table 1 shows the 2θ values and crystallite size determined for different (h,k,l) planes as observed from the XRD patterns for as synthesized ZnS sample and calcinated mixed phase (ZnS+ ZnO) at 700 oC.

Figure 3C shows the FTIR spectra of ZnS sample after calcinations. Significant vibration peaks are observed at 669, 1128, 2341, 2361cm^{-1} and small peaks are also observed at 1636 and 3371cm^{-1}. The decrease in intensity of peaks obtained at 1340 and

2341cm^{-1} signifies that part of the adsorbed atmospheric CO2 gets desorbed from the surface of calcinized ZnS sample. The absence of peaks in the range of 3000-3600cm^{-1} indicates the desorption of adsorbed water molecules from the surface of calcinized ZnS sample.

Table 1: The as measured values of 2θ and Grain size for different (hkl) planes from XRD patterns for ZnS before calcination and the ZnS* and ZnO· mixed phase after calcination at 700 °C.

	Plane	2θ	Grain Size (Å)
ZnS as Synthesized	(111)*	28.73°	22.6
	(220)*	48.02°	33.5
	(311)*	56.90°	53.6
Calcinated (ZnS* + ZnO·) Mixed Phase	(105)*	32°	208
	(106)*	34.7°	215
	(101)·	36.5°	221
	(102)·	47.9°	264
	(110)·	56.8°	322
	(103)·	63.1°	393
	(112)·	68.2°	478
	(004)·	72.8°	506

Figure 3D displays the photoluminescence spectra of the calcinized ZnS sample. As shown in the Figure, the plot contains two peaks at 337.4 and 490.6nm for ZnS sample after calcinations. Appearance of a broad peak centered at 490.6nm can be attributed to the presence of oxygen vacancy defects [35], which suggests that ZnS sample is partly oxidized to ZnO during calcinations. The other peak at 337.4nm is due to the band to band transition of ZnS. There is also significant increase in the photoluminescence intensity of the calcinized ZnS sample, which makes it compactable for vast array in luminescence based applications.

Conclusion

In this paper, we have successfully demonstrated a simple cost-effective green synthetic protocol for the preparation of honey mediated cubic zinc blend structured ZnS nano/micro particles with band gap energy 4.08eV. The structural and morphological properties of zinc sulphide nano/microstructures were studied by X-ray diffraction, scanning electron microscope, energy dispersive X-rays spectroscopy and Fourier transform infra-red spectroscopy. It can exhibit a phase transformation to hexagonally packed wurzite structured ZnS (3.37eV) after calcinations at 700 oC as demonstrated by XRD studies. Partial oxidation to ZnO after calcinations has lead to increase in the photoluminescence intensity which makes it compatible for vast array in luminescence based applications.

Acknowledgement

BA thanks to the Board of College and University Development (BCUD), (BCUD, Finance/2013-14/1776/ dated: 20/01/2014 and BCUD, Finance/2016-17/1596/ dated: 08/11/2016), University of Pune for provision of financial support. UKS would also like to thank INSA, New Delhi (SP/VF-9/2014-15/273 1st April, 2014) for INSA visiting Scientist Fellowship for 2014-2015 under the supervision of BA at Bio-Inspired Materials Research Laboratory, Department of Chemistry, Savitribai Phule Pune University, (Formerly University of Pune) Ganeshkhind, Pune-411007, India.

References

1. Davidson WL, Shull CG, Wollan EO, Morton GA (1948) Range of nuclear forces in the neutron-proton triplet interaction. Phys Rev 73: 262.
2. Peng WQ, Cong GW, Qu SC, Wang ZG (2006) Synthesis and photoluminescence of ZnS: Cu nanoparticles. Opt Mater 29(2-3): 313-317.
3. Fang X, Zhai T, Gautam UK, Li L, Wu L, et al. (2011) ZnS nanostructures: From synthesis to applications. Prog Mater Sci 56(2): 175-287.
4. Dutková E, Baláž P, Pourghahramani P, Velumani S, Ascencio JA, et al. (2009) Properties of Mechanochemically Synthesized ZnS Nanoparticles.J Nanosci Nanotechnol 9(11): 6600-6605.
5. Saravanan N, Teh GB, Yap SYP, Cheong KM (2008) J Mater Sci Mater Electron 19: 1206.
6. Borah JP, Barman J, Sarma KC (2008) Structural and optical properties of zns nanoparticles. Chalcogenide Lett 5(9): 201-208.
7. Yeh CY, Lu ZW, Froyen S, Zunger A (1992) Zinc-blende-wurtzite polytypism in semiconductors. Phys Rev B Condens Matter 46: 10086-10097.
8. Yao WT, Yu SH, Pan L, Li J, Wu QS, et al. (2005) c-kit expression in small cell carcinoma of the urinary bladder: prognostic and therapeutic implications. Mod Pathol 18(3): 320-323.
9. Chai L, Du J, Xiong S, Li H, Zhu Y, et al. (2007) Synthesis of wurtzite zns nanowire bundles using a solvothermal technique. J Phys Chem 111(34): 12658-12662.
10. Huang MW, Cheng YW, Pan KY, Chang CC, Shieu FS, et al. (2012) Appl Surf Sci 261: 665.
11. Shanmugam N, Cholan S, Sundaramanickam A, Viruthagiri G, Kannadasan N, et al. (2013) Walailak J Sci & Tech 10: 149.
12. Manoharan SS, Goyal S, Rao ML, Nair MS, Pradhan A, et al. (2001) Mater Res Bull 36: 1039.
13. Limaye MV, Gokhale S, Acharya SA, Kulkarni SK (2008) Template-free zns nanorod synthesis by microwave irradiation. Nanotechnology 19(41): 415602.
14. Pathak CS, Mishra DD, Agarawala V, Mondal MK (2012) Indian J Phys 86**:** 777.
15. Shivshankar S, Rai A, Ahmad A, Sastry M (2004) Rapid synthesis of Au, Ag, and bimetallic Au core-Ag shell nanoparticles using Neem (Azadirachta indica) leaf broth. J Colloid Interface Sci 275(2): 496-502.
16. Sastry M, Ahmad A, Khan IM, Kumar R (2003) Biosynthesis of metal nanoparticles using fungi and actinomycete. Curr Sci 85(2): 162-170.
17. Ankamwar B, Mandal G, Sur UK, Ganguly T (2012) An effective biogenic protocol for room temperature one-step synthesis of defective nanocrystalline silver nanobuns using leaf extract. Digest J Nano Biostruc 7(2): 599-605.
18. Shankar SS, Rai A, Ankamwar B, Singh A, AhmadA, et al. (2004) Biological synthesis of triangular gold nanoprisms. Nature Mater 3(7): 482-488.
19. Ankamwar B, Chaudhary M, Sastry M (2005) Gold Nanotriangles Biologically Synthesized using Tamarind Leaf Extract and Potential Application in Vapor Sensing. Syn React Inorg Metal Org Nano-Metal Chem 35(1): 19-26.

20. Ankamwar B, Damle C, Ahmad A, Sastry M (2005) Biosynthesis of gold and silver nanoparticles using Emblica Officinalis fruit extract, their phase transfer and transmetallation in an organic solution. J Nanosci Nanotech 5(10): 1665-1671.

21. Philip D (2009) Honey mediated green synthesis of gold nanoparticles. Spectrochim Acta A Mol Biomol Spectrosc 73(4): 650-653.

22. Philip D (2010) Honey mediated green synthesis of silver nanoparticles. Spectrochim Acta A Mol Biomol Spectrosc 75(3) 1078-1081.

23. Venu R, Ramulu TS, Anandakumar S, Rani VS, Kim CG, et al. (2011) Bio-directed synthesis of platinum nanoparticles using aqueous honey solutions and their catalytic applications. Colloids Surf A38 4(1-3): 733-738.

24. Reddy SM, Datta KKR, Sreelakshmi CH, Eswaramoorthy M, Reddy BVS, et al. (2012) Honey Mediated Green Synthesis of Pd Nanoparticles for Suzuki Coupling and Hydrogenation of Conjugated Olefins. Nanosci Nanotechnol Lett 4(4): 420-425.

25. Senapati US, Sarkar D (2014) Indian J Phys 88: 557.

26. Ummartyotin S, Bunnak N, Juntaro J, Sain M, Manuspiya H, et al. (2012) Synthesis and luminescence properties of ZnS and metal (Mn, Cu)-doped-ZnS ceramic powder. Solid State Sci. 14(3): 299-304.

27. Klung HP, Alexander LE (1974) X-ray Diffraction Procedures for Polycrystalline and Amorphous Materials. In: (2nd edn), Wiley, New York, 79(6): 553.

28. Mahajan CM, Takwale MG (2014) J Alloys Compd 584: 128.

29. Tolia J, Chakraborty M, Murthy ZVP (2011) IPCBEE 24: 489.

30. Murugadoss G, Kumar MR (2014) Nanotechnology. Appl Nanosci 4: 67.

31. Devi BSR, Raveendran R, Vaidyan AV (2007) Synthesis and characterization of Mn^{2+}-doped ZnS nanoparticles. Pramana J. Phys 68(4): 679-687.

32. Koo J, Cho JJ, Yang JH, Yoo PJ, Oh KW, et al. (2012) Bull Korean Chem Soc 33: 636.

33. Ankamwar BG, Kamble VB, Annsi JI, Sarma LS, Mahajan CM, et al. (2016) J Nanosci Nanotech 16**:** XX-XX**.**

34. Mahajan CM, Takwale MG (2013) Curr Appl Phys 13: 2109.

35. Irimpan L, Nampoori VPN, Radhakrishnan P, Deepthy A, Krishnan B, et al. (2007) Size dependent fluorescence spectroscopy of nanocolloids of ZnO. J Appl Phys 102**:** 063524.